JOURNAL OF SOLID STATE CHEMISTRY **137,** 28–32 (1998)
ARTICLE NO. SC977656

Synthesis of Manganese Oxides by Reduction of $KMnO_4$ with KBH_4 in Aqueous Solutions

C. Tsang, J. Kim, and A. Manthiram[1]

Center for Materials Science & Engineering, ETC 9.104, University of Texas at Austin, Austin, Texas 78712

Received September 5, 1996; in revised form August 18, 1997; accepted October 12, 1997

Reduction of $KMnO_4$ with KBH_4 in aqueous solutions has been investigated systematically at ambient temperatures as a function of reaction pH and the volume of borohydride. The products are characterized by X-ray diffraction, transmission electron microscopy, atomic absorption spectroscopy, redox titrations to determine the oxidation state of manganese, and thermogravimetric analysis. The reduction gives both binary $MnO_{2-\delta}$ and ternary $K_xMn_yO_z$ oxides that are hydrated and nanocrystalline. The composition of the reduction products is influenced by the reaction pH as well as the volume of borohydride. While acidic conditions tend to stabilize products with predominantly Mn^{4+} due to a disproportionation of Mn^{3+}, nearly neutral conditions could access Mn^{3+} with $\delta \approx 0.5$ in $MnO_{2-\delta}$. While no potassium-containing $K_xMn_yO_z$ is obtained in highly acidic solutions with pH ≈ 1, the compound becomes accessible with increasing pH, and a maximum $x \approx 0.5$ could be obtained in highly basic solutions with pH ≈ 11. The as-prepared samples lose most of the water below 200°C and tend to lose oxygen at higher temperatures. © 1998 Academic Press

1. INTRODUCTION

Manganese oxides are widely used as electrode materials in both primary and secondary batteries. For example, they are used in Leclanche, alkaline, and lithium cells (1–7). A higher cell voltage (>3 V) and lower cost make the manganese oxides particularly attractive for battery applications. However, the electrochemical performance of the manganese oxides is strongly controlled by powder morphology, particle size, composition, and crystal structure. In addition, the manganese oxides are known to undergo structural and compositional changes as they are heated to moderate temperatures ($T \sim 400$°C) (8). For example, one of the most widely used oxides, γ-MnO_2, is metastable and decomposes to Mn_2O_3 at $T > 450$°C. Also, it is very difficult to remove all the surface and occluded water from γ-MnO_2, which is generally obtained electrolytically (EMD) or by chemical methods (CMD). These considerations have fueled some efforts in recent years to develop low-temperature synthesis procedures for obtaining manganese oxides. For example, (i) extraction of Li from the spinel oxide $LiMn_2O_4$ (9–11) and the rocksalt phase Li_2MnO_3 (12) with sulfuric acid; (ii) reduction of permanganate with fumaric acid (13), sugar (14), hydrochloric acid (15, 16), and Mn^{2+} (17), and (iii) oxidation of Mn^{2+} (18) have been investigated.

We recently showed (19) that alkali metal borohydrides ABH_4 (A = Na, and K) can be used to reduce oxo ions $(MO_4)^{n-}$ (M = V, Mo, and W) in aqueous solutions to obtain MO_2 binary oxides and $A_xM_yO_z$ ternary oxides. Some of these binary oxides were found to be attractive as electrode materials for lithium batteries (20, 21). A more systematic investigation of the molybdate (22, 23) and tungstate (24), systems reveals that the volume and concentration of the borohydride, the reaction pH, and the degree of condensation of the metalate ions strongly influence the composition of the products. We report in this paper a systematic investigation of the reduction of $KMnO_4$ with KBH_4 in aqueous solutions with an aim to obtain manganese oxides.

2. EXPERIMENTAL

Reduction reactions were carried out at various pH values by reducing a fixed volume (50 ml) of 0.1 M $KMnO_4$ solution with varying volumes of 0.25 M KBH_4 solutions. The $KMnO_4$ solution was prepared by dissolving the required amount of $KMnO_4$ in deionized water. The 0.25 M KBH_4 solution was prepared by dissolving the required quantities of KBH_4 in dilute KOH solution with a pH of 11–12. The initial pH needs to be maintained high in order to prevent the rapid loss of hydrogen before the reduction reaction, as the hydrolysis of borohydrides is facilitated by acidic conditions (25)

$$BH_4^- + 2H_2O \rightarrow BO_2^- + 4H_2. \qquad [1]$$

Typically, the reactions were carried out by adding a specific volume of the borohydride from a burette to the

[1]To whom correspondence should be addressed.

0022-4596/98 $25.00

permanganate solution, which was kept under constant stirring at a predetermined pH. As the pH tends to rise due to the formation of the basic KBO_2 and KOH (see reaction [2] below), concentrated HCl was added during the reduction process to maintain constant pH. The solid product obtained after the reduction was filtered, washed several times, and air-dried at room temperature.

Crystal–chemical characterizations were carried out with X-ray powder diffraction and transmission electron microscopy (TEM). Qualitative and quantitative elemental analyses were carried out, respectively, with a scanning electron microscope (SEM) equipped with an energy dispersive spectrometer (EDS) and with atomic absorption spectroscopy (AAS). The oxidation state of manganese and the oxygen content were determined by a potentiometric redox titration employing vanadyl sulfate (26). Compositional changes with temperatures were investigated by thermogravimetric analysis (TGA).

3. RESULTS AND DISCUSSION

Reduction experiments were carried out at four different pH values (1, 3, 6, and 11) with 50 ml of 0.1 M $KMnO_4$ and varying amounts of 0.2 M KBH_4, as given in Table 1. The as-prepared samples show no discernible reflections in the X-ray diffraction pattern (Fig. 1a). However, selected area diffraction in TEM shows diffraction spots or rings (Fig. 2), indicating that the as-prepared samples are nanocrystalline and not amorphous. This is in contrast to the as-prepared samples in the molybdate and tungstate systems, which were found to be amorphous (22–24).

For further characterization, the samples were heated in a thermogravimetric analyzer. The TGA plot for sample 2 in Table 1, for example, is shown in Fig. 3a. The sample shows about 13% weight loss below 200°C, a small, gradual weight loss in the range 200–450°C, and a small, sharp weight loss around 470°C. To understand the origin of these weight losses, the sample was heated to various temperatures (200, 450, and 600°C) in TGA, and the products were analyzed for the oxidation state of manganese. Both EDS analysis and AAS analysis show no potassium in sample 2. The oxidation state analysis and the observed weight loss, were used to determine the compositions at different temperatures, as indicated in the TGA plot of Fig. 3a. The results suggest that predominantly water is lost below 200°C, while both water and oxygen are lost in the intermediate region 200–450°C. The sharp weight loss at around 470°C corresponds only to oxygen.

The compositions of the as-prepared samples calculated from the results of AAS, oxidation state analysis, and TGA data are given in Table 1 for all the samples. The general shape of the TGA curves for samples 1, 4, 5, and 9, each having a manganese oxidation state of $>3.58+$ and no potassium is similar to the plot of sample 2 in Fig. 3a. On the other hand, sample 6 in Table 1 with a manganese oxidation state close to $3+$ and no potassium, shows a difference in the TGA plot (Fig. 3b). The constancy of weight in the intermediate region 200–350°C appears to be due to a balance between the loss of remaining water and a slight oxidation of the already-reduced sample, which has a lower oxidation state for manganese. The small, gradual weight loss above 400°C corresponds to the loss of a small amount of oxygen. Also, the potassium-containing samples 3, 7, and 8 (Fig. 3c) show a small difference in the TGA plot compared to the samples containing no potassium, such as sample 2 in Fig. 3a. The potassium-containing samples tend to be more stable, with a manganese oxidation state of $>3.5+$, even after heating to 600°C. The sharp oxygen loss in these samples does not begin to occur until above 550°C compared to 450°C in sample 2.

TABLE 1
Reduction of 50 ml of 0.1 M $KMnO_4$ (5 mmol) with Varying Amounts of 0.25 M KBH_4 at Varying pH

Sample number	pH	Amount of KBH_4		As-prepared samples			Crystalline products identified after heating in evacuated, sealed silica tube at 550°C for 2 days[a]
		ml	mmol	Composition $K_xMn_yO_z$	Water content (nH_2O)	Oxidation state of manganese	
1	1	3	0.75	$MnO_{1.84}$	0.76	3.68 +	MnO(100)
2	1	20	5.0	$MnO_{1.89}$	0.79	3.78 +	Mn_2O_3(100)
3	3	10	2.5	$K_{0.14}MnO_{2.05}$	1.15	3.97 +	$K_{2-x}Mn_8O_{16}$(70), Mn_2O_3(30)
4	3	30	7.5	$MnO_{1.85}$	0.86	3.69 +	Mn_2O_3(100)
5	6	3	0.75	$MnO_{1.88}$	1.27	3.76 +	MnO(100)
6	6	20	5.0	$MnO_{1.53}$	0.31	3.05 +	Mn_3O_4(100)
7	11	3	0.75	$K_{0.48}MnO_{2.24}$	1.62	3.99 +	$K_2Mn_4O_8$(90), Mn_3O_4(10)
8	11	10	2.5	$K_{0.54}MnO_{2.26}$	1.74	3.99 +	$K_2Mn_4O_8$(95), Mn_3O_4(5)
9	11	28	7.0	$MnO_{1.79}$	0.69	3.58 +	Mn_2O_3(40), Mn_3O_4(60)

[a] Numbers in parentheses refer to relative amounts of the phases calculated from X-ray diffraction intensities.

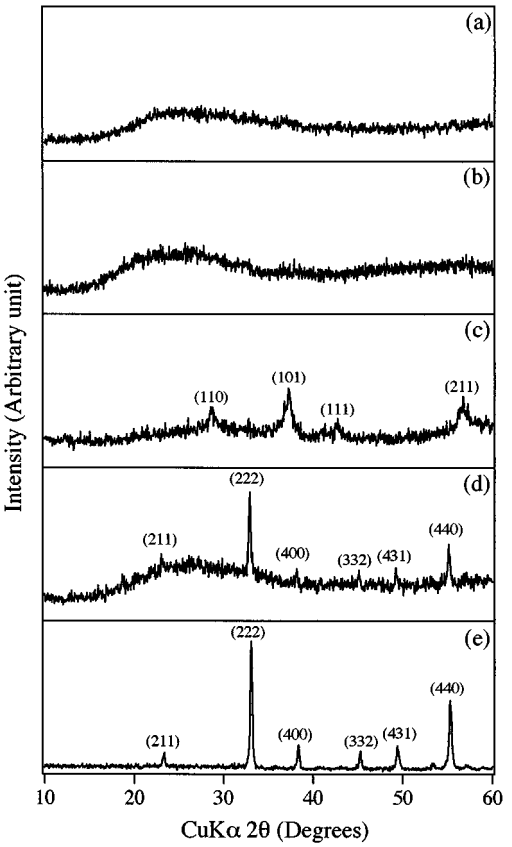

FIG. 1. X-ray powder diffraction patterns of sample 2 in Table 1: (a) as-prepared sample; (b) after just heating to 450°C in TGA; (c) after holding at 400°C in TGA for 15 h (MnO_2); (d) after just heating to 600°C in TGA (Mn_2O_3); and (e) after heating in an evacuated, sealed silica tube at 550°C for 2 days (Mn_2O_3).

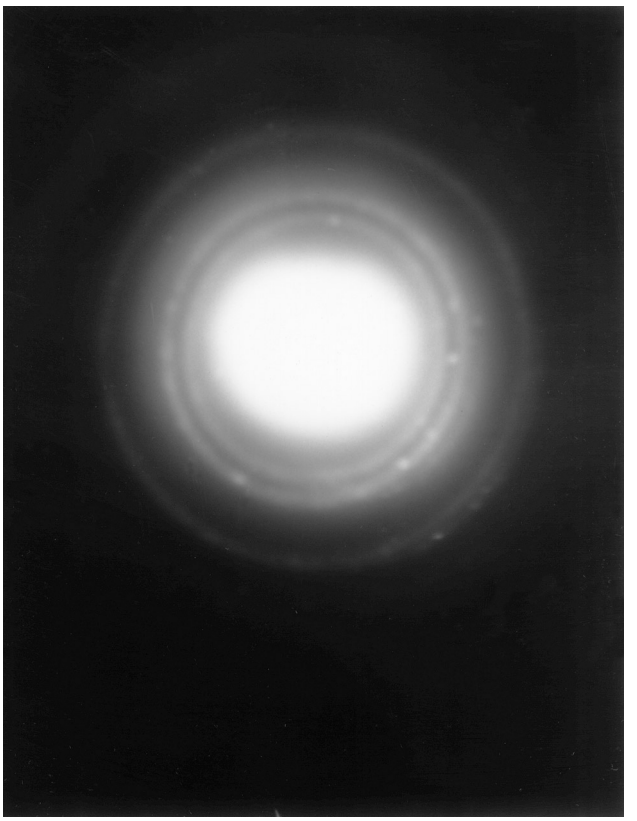

FIG. 2. Selected area diffraction pattern recorded in TEM sample 6 in Table 1.

To characterize the crystal chemistry, X-ray powder diffraction patterns were also recorded after heating to various temperatures. The results are shown, for example, in Fig. 1 for sample 2. Although heating briefly to 450°C in TGA at a heating rate of 10°C does not show any discernible reflections, holding in TGA at, for example, 400°C for about 15 h shows broad reflections corresponding to β-MnO_2 (pyrolusite). Also, heating at around 250°C for 15 h gives the metastable phase, ε-MnO_2 (akkhtensite) (26, 27), which begins to transform irreversibly above 300°C into the more stable pyrolusite. On the other hand, either only heating to 600°C in TGA or heating in an evacuated, sealed silica tube at 550°C for 2 days shows reflections corresponding to Mn_2O_3 (bixbyite) due to the loss of oxygen. It is interesting to note that even in a closed system such as the sealed silica tube, the sample loses oxygen at higher temperatures to give Mn_2O_3. The loss of oxygen at higher temperatures (550°C) in evacuated, sealed silica tubes and the formation of more reduced phases were also observed in all cases, as revealed by the phase identification given in Table 1. MnO_2 is known to give progressively, Mn_2O_3, Mn_3O_4, and MnO upon heating to temperatures greater than 450°C. The reduction in sealed tubes was found to be more severe, giving a much more reduced phase MnO with a green color for samples prepared with a smaller amount of borohydride, such as samples 1 and 5 in Table 1. We believe the fine nature (smaller particle size) of the solid formed with a smaller amount of borohydride results in a much easier reduction in the evacuated, sealed silica tubes. The potassium-containing samples heated at 550°C in sealed tubes give either $K_{2-x}Mn_8O_{16}$ (cryptomelane having the hollandite structure) (28) or $K_2Mn_4O_8$ (29), depending on the potassium content in the reduction product.

Based on the compositions obtained for the as-prepared samples in Table 1, we can now write a general chemical reaction for the formation of the reduction products:

$$\begin{aligned} &KMnO_4 + KBH_4 + (1 - x - \delta)H_2O \\ &\quad \rightarrow KBO_2 + K_xMnO_{2-\delta} + (1 - x)KOH \\ &\qquad + (2.5 - 0.5x - \delta)H_2. \end{aligned} \quad [2]$$

Several points can be recognized based on the compositions found for the as-prepared samples in Table 1. Under acidic conditions with pH $\leq$ 3, the average oxidation state of

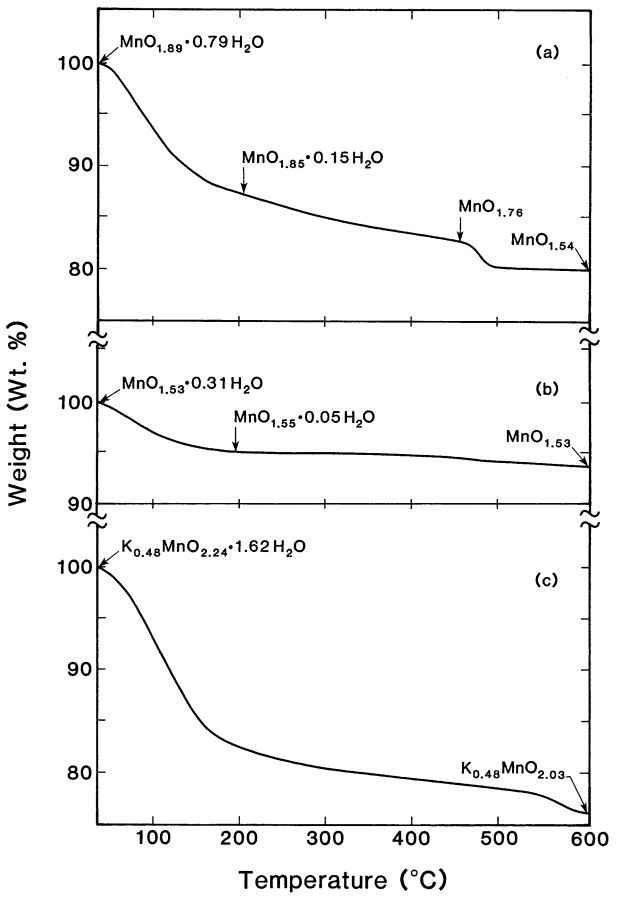

FIG. 3. TGA plots of (a) sample 2, (b) sample 6, and (c) sample 7 in Table 1 recorded with 10°C/min under a flowing atmosphere of 70% nitrogen and 30% oxygen.

manganese in the reduction product is $\geq 3.68+$, which is consistent with the fact than Mn^{3+} tends to disproportionate in acid to give Mn^{4+} in the solid, and Mn^{2+} in solution (9). On the other hand, under nearly neutral conditions with pH $\sim$6, a much lower oxidation state of close to $3+$ can be achieved, as Mn^{3+} can be stable in neutral solutions. Also, the oxidation state of manganese in the reduction product obtained at pH 6 decreases with increasing amounts of borohydride due to increasing reducing power. However, such a trend is not readily apparent under highly acidic conditions with pH 1. This is because (i) a higher reducing power of borohydride under acidic conditions, arising from increasing facilitation of the hydrolysis reaction [1], causes a stronger reduction even with a smaller amount of borohydride, and (ii) an instability and disproportionation in acid of Mn^{3+} formed on adding more borohydride. This conclusion is also supported by the fact that solid formed begins to dissolve above about 20 ml of borohydride, and no solid is obtained above 30 ml of borohydride.

The tendency to form potassium-containing samples increases with increasing pH. For example, with a constant borohydride volume of 3 ml, no potassium is found in samples 1 and 6 obtained at pH ≤ 6, whereas a significant amount of potassium is found in sample 7 obtained at pH 11. Thus, the highest potassium content of about 0.5 per Mn could be achieved only under basic conditions. Also, it was noticed generally that at a given pH, the amount of potassium in the reduction product increases initially with an increasing volume of borohydride, reaches a maximum at an intermediate volume, and then decreases. For example, at pH 3, no potassium is found in the product at both 3 and 30 ml (sample 4) of borohydride, but a small amount of potassium is found at 10 ml (sample 3) of borohydride. Similarly at pH 11, the potassium content increases slightly between 3 and 10 ml of borohydride, and no potassium is found at 28 ml. These results suggest that a complex interplay between the contents of the reaction medium and the stability of the product formed is at work in determining the composition of the products. In addition, it is found that the incorporation of potassium into the products tends to stabilize a manganese oxidation state close to $4+$.

4. CONCLUSIONS

The reduction of $KMnO_4$ with KBH_4 in aqueous solutions at ambient temperatures has been investigated systematically. Both hydrous, binary oxides $MnO_{2-\delta}$ and hydrous ternary oxides $K_xMn_yO_z$ are obtained depending on the reaction pH and the amount of borohydride. While acidic conditions (pH ≤ 3) tend to stabilize predominantly Mn^{4+} with $\delta < 0.16$ in $MnO_{2-\delta}$, nearly neutral conditions (pH $\sim$6) can stabilize Mn^{3+} with δ as high as 0.47 in $MnO_{2-\delta}$. The potassium content that can be incorporated into $K_xMn_yO_z$ increases with increasing pH, and a maximum potassium content $x = 0.54$ is achieved at pH 11. Although the as-prepared samples do not show any discernible reflections in X-ray diffraction, TEM shows them to be nanocrystalline. The hydrous oxides lose most of the water below 200°C and tend to lose oxygen at higher temperatures. Prolonged annealing at $T > 200$°C leads to particle growth and development of diffraction lines in X-ray patterns. The nanocrystalline nature of the products may become attractive for battery electrodes. Nanocrystalline and amorphous electrodes are known to exhibit electrochemical behavior different from that of their conventional crystalline analogs with larger particle size (20, 30). We plan to investigate the electrochemical properties of these nanocrystalline manganese oxides in the near future.

ACKNOWLEDGMENTS

Financial support by the National Science Foundation Grant DMR-9401999 and the Welch Foundation Grant F-1254 is gratefully acknowledged.

REFERENCES

1. R. Huber, K. V. Kordesch, A. Kozawa, and D. B. Wood, in "Batteries," Vol. 1, "Manganese Dioxide" (K. V. Kordesch, Ed.), Dekker, New York (1974).
2. G. Pistoia, *J. Electrochem. Soc.* **129,** 1861 (1982).
3. F. W. Dampier, *J. Electrochem. Soc.* **121,** 656 (1974).
4. M. Beltowska-Brzezinska, E. Dutkiewicz, and J. Stuczyniska, *J. Electroanal. Chem.* **135,** 103 (1982).
5. J. C. Nardi, *J. Electrochem. Soc.* **132,** 1787 (1985)
6. M. M. Thackeray, W. I. F. David, P. G. Bruce, and J. B. Goodenough, *Mater. Res. Bull.* **18,** 461 (1983).
7. D. Guyomard and J. M. Tarascon, *J. Electrochem. Soc.* **139,** 937 (1992).
8. H. Ikeda, U.S. Patent 4,133,856.
9. J. C. Hunter, *J. Solid State Chem.* **39,** 142 (1981).
10. M. M. Thackeray and A. De Kock, *J. Solid State Chem.* **74,** 414 (1988).
11. M. M. Thackeray, A. De Kock, L. A. De Picciotto, and G. Pistoia, *J. Power Sources* **26,** 355 (1989).
12. M. H. Rossouw, D. C. Liles, and M. M. Thackeray, *J. Solid State Chem.* **104,** 464 (1993).
13. S. Bach, M. Henry, N. Baffier, and J. Livage, *J. Solid State Chem.* **88,** 325 (1990).
14. S. Ching, J. A. Landdrigan, M. L. Jorgensen, N. Duan, S. L. Suib, and C. L. O'Young, *Chem. Mater.* **7,** 1064 (1995).
15. M. Tsuji, S. Komarneni, Y. Tamaura, and M. Abe, *Mater. Res. Bull.* **27,** 741 (1992).
16. F. Leroux, D. Guyomard, and Y. Piffard, *Solid State Ionics* **80,** 299 (1995).
17. R. N. DeGuzman, Y. F. Shen, E. J. Neth, S. L. Suib, C. L. O'Young, S. Levine, and J. M. Newsam, *Chem. Mater.* **6,** 815 (1994).
18. P. Strobel and J. C. Charenton, *Rev. Chim. Miner.* **23,** 125 (1986).
19. A. Manthiram, A. Dananjay, and Y. T. Zhu, *Chem. Mat.* **6,** 1601 (1994).
20. A. Manthiram and C. Tsang, *J. Electrochem. Soc.* **143,** L143 (1996).
21. C. Tsang and A. Manthiram, *J. Electrochem. Soc.* **144,** 520 (1997).
22. C. Tsang, A. Dananjay, J. Kim, and A. Manthiram, *Inorg. Chem.* **35,** 504 (1996).
23. C. Tsang and A. Manthiram, *J. Mater. Chem.* **7,** 1003 (1997).
24. C. Tsang, S. Y. Lai, and A. Manthiram, *Inorg. Chem.* **36,** 2206 (1997).
25. H. I. Schlesinger, H. C. Brown, A. E. Finholt, J. R. Gilbreath, H. R. Hoekstra, and E. K. Hyde, *J. Amer. Chem. Soc.* **75,** 215 (1953).
26. C. Tsang and A. Manthiram, *Solid State Ionics* **89,** 305 (1996).
27. JCPDS Card 30-0820, Joint Committee on Powder Diffraction Standards, Swarthmore, PA.
28. JCPDS Card 44-1386, Joint Committee on Powder Diffraction Standards Swarthmore, PA.
29. JCPDS Card 16-0205, Joint Committee on Powder Diffraction Standards Swarthmore, PA.
30. S. Y. Huang, L. Kavan, I. Exnar, and M. Gratze, *J. Electrochem. Soc.* **142,** L142 (1995).